

Generation of Mutated Variants of the Human Form of the MHC Class I-related Receptor, FcRn, with Increased Affinity for Mouse Immunoglobulin G

Jinchun Zhou^{1,2}, James E. Johnson^{1,2}, Victor Ghetie²
Raimund J. Ober² and E. Sally Ward^{1,2*}

¹Center for Immunology
University of Texas
Southwestern Medical Center
6000 Harry Hines Blvd, Dallas
TX 75390-9093, USA

²Cancer Immunobiology Center
University of Texas
Southwestern Medical Center
6000 Harry Hines Blvd, Dallas
TX 75390-9093, USA

Much data support the concept that the MHC class I-related receptor FcRn serves to regulate immunoglobulin G (IgG) concentrations in serum and other diverse body sites in both rodents and humans. Previous studies have indicated that the human ortholog of FcRn is endowed with unexpectedly high stringency in binding specificity for IgGs. In contrast to mouse FcRn, which binds promiscuously to IgGs across species, human FcRn does not bind to mouse IgG1 or IgG2a, and interacts weakly with mouse IgG2b. Here, we investigate the molecular basis for this high-level specificity. We have systematically mutated human FcRn residues to the corresponding mouse FcRn residues in the regions that encompass the FcRn–IgG interaction site. Notably, mutation of the poorly conserved residue Leu137 of human FcRn to glutamic acid (L137E) generates a human FcRn mutant that binds to mouse IgG1 and mouse IgG2a with equilibrium dissociation constants of 13.2 μ M and 14.4 μ M, respectively. From earlier high-resolution structural analyses of the rat FcRn–rat Fc complex, residue 137 of human FcRn is predicted to contact residue 436 of IgG, which can be either His436 (mouse IgG1, mouse IgG2a) or Tyr436 (human IgG1, mouse IgG2b). The simplest interpretation of our data for the L137E mutant is therefore that replacement of the Leu137–Tyr436 (human) by the Glu137–His436 (mouse) pair generates a receptor that can bind to mouse IgG1 and mouse IgG2a. The L137E mutation reduces the affinity of human FcRn for human IgG1 by about twofold, consistent with the introduction of a less favorable Glu137–Tyr436 interaction. However, the analysis of the effects of other mutations on the binding to different IgGs indicates that the contribution to binding of the interaction of FcRn residue 137 with IgG residue 436 can vary. This suggests the existence of distinct docking topologies that are accompanied by variations in contacts between these two residues for different FcRn–IgG pairs. Our observations are of direct relevance to understanding the molecular nature of the human FcRn–IgG interaction. In turn, understanding human FcRn function has significance for the optimization of the serum half-lives of therapeutic and prophylactic antibodies.

© 2003 Elsevier Ltd. All rights reserved.

Keywords: neonatal Fc receptor FcRn; immunoglobulin G; site-directed mutagenesis; surface plasmon resonance; serum half-life

*Corresponding author

Introduction

Abbreviations used: FcRn, neonatal Fc receptor; IgG, immunoglobulin G; K_D , equilibrium dissociation constant; β_2 m, β_2 -microglobulin; SPR, surface plasmon resonance.

E-mail address of the corresponding author:
sally.ward@utsouthwestern.edu

The MHC class I-related receptor FcRn was identified initially in rodents as the receptor that transports immunoglobulin G (IgG) from maternal milk to the bloodstream of the neonate^{1,2} via a process called transcytosis. FcRn is therefore an IgG

transporter. More recent studies have shown that this receptor has diverse functions, including the regulation of serum IgG levels in mice.^{3–5} FcRn appears to carry out these functions by binding to IgGs and transporting them within (recycling) or across cells (transcytosis). Following uptake into FcRn-expressing cells, IgGs are hypothesized to enter acidic vesicles, where they have the opportunity to interact with FcRn at a pH (6.0–6.5) that is permissive for the FcRn–IgG interaction.⁶ IgG molecules that do not bind to FcRn enter the lysosomal pathway and are degraded.⁷ By this mechanism, FcRn can serve several roles that are not mutually exclusive: first, it can act to transfer IgG *via* transcytosis across endothelial and epithelial barriers of diverse origin.^{1,2,8–14} In some cases, such as in the lactating mammary gland, FcRn may regulate the levels of IgG delivered into milk by both transcytosis and recycling.¹⁵ Second, FcRn expression in endothelial cells appears to regulate the levels of IgG in the serum^{3–5,16} by trafficking pathways that most likely involve a combination of transcytosis and recycling.¹⁷ FcRn therefore serves to control the levels of IgG at diverse body sites and has a much broader role in humoral immunity than originally believed.

A human ortholog of rodent FcRn has been isolated from placental syncytiotrophoblast,¹⁸ and FcRn expression at the protein level has been demonstrated.^{19–21} Studies using an *ex vivo* placental transport model have shown that, as in rodents, binding of IgG to FcRn is essential for transport across the placenta.²² In addition, IgGs that do not bind to human FcRn accumulate in lysosomes in FcRn-expressing endothelial cells.⁷ Thus, the function of FcRn in humans appears to be broadly similar to that in rodents, although ethical constraints preclude direct testing of this hypothesis. However, data from both analyses of FcRn trafficking in transfected epithelial cells^{9,23} and binding studies with recombinant FcRn²⁴ indicate that there are cross-species differences. Here, we focus on the differences in binding specificity of human *versus* mouse FcRn. Our studies therefore have direct relevance to the engineering of antibodies for the optimization of FcRn-mediated functions.

The interaction site for FcRn on IgG (human and rodent) has been mapped and shown to encompass conserved residues at the CH2–CH3 domain interface.^{25–29} These residues include Ile253, His310 and His435. The involvement of IgG histidine residues in binding regulates the pH-dependence of the interaction, resulting in much stronger binding at pH 6.0–6.5 relative to that at pH 7.3. This pH-dependence provides a mechanism by which IgG can be bound to FcRn in endosomes and released at near-neutral pH,¹⁷ facilitating the role of FcRn as a transporter. The importance of pH-dependence in the FcRn–IgG interaction has been demonstrated recently in a study in which genetically manipulated IgGs that bind to FcRn with reduced pH-dependence have lower serum half-lives in mice.³⁰

Despite the apparent similarity of the docking site for FcRn on IgG across species, a recent comparison of the binding of human and mouse FcRn to IgG molecules from different species showed marked differences in specificity:²⁴ mouse FcRn is highly promiscuous and binds to IgGs of every species analyzed (mouse, rat, human, bovine, sheep, guinea pig), whereas human FcRn is much more selective and binds to only a subset of these IgGs. Human FcRn does not, for example, bind with a measurable affinity to mouse IgGs (with the exception of mouse IgG2b). The poor binding of human FcRn to mouse IgG1 explains the long misunderstood phenomenon that mouse IgG1 is cleared rapidly from the human circulation.^{31,32}

In the current study we have attempted to understand the molecular basis for the difference in specificity of human and mouse FcRn for IgG. This has been carried out by mutating human FcRn residues that are not well conserved across species to the corresponding mouse FcRn amino acids. The mutated residues are known from X-ray crystallography to be either involved directly in the rodent FcRn–IgG interaction or in close proximity to the interaction site.²⁹ Mutated human FcRn variants have been expressed in recombinant form and their binding to human IgG1 and mouse IgG isotypes assessed using surface plasmon resonance (SPR). Using this approach, we have been able to locate a primary determinant of the differential binding specificity to an individual amino acid residue in the $\alpha 2$ domain of FcRn. We have observed that, in some cases, the mutations can have effects that cannot be explained using the existing X-ray structure of rat FcRn complexed with rat Fc²⁹ as a model. Thus, FcRn–IgG interactions may differ in topology across species and IgG isotypes.

Results

Variations between human and rodent FcRn sequences and generation of mutants

To determine the molecular basis for the difference in binding specificity of human *versus* mouse FcRn for IgGs, selected regions or residues of human FcRn were mutated to the corresponding sequences in mouse FcRn^{18,33} (Tables 1 and 2; Figure 1). In the X-ray crystallographic structure of rat FcRn (highly homologous to mouse FcRn^{33,34}) complexed with rat Fc (IgG2a derived), the mutated residues either contact directly, or are in close proximity to, IgG ligand (Table 2; Figure 2).²⁹ The most notable difference between human and mouse FcRn is the non-conservative change of Leu137 (human) to Glu137 (mouse) (for simplicity, in the current study the two amino acid deletion in human FcRn is ignored in the residue numbering, which corresponds to the homology alignment of rodent and human FcRn^{18,33} (Figure 1)). In the complex of rat FcRn and rat Fc,

Table 1. Oligonucleotides used to generate mutations of human FcRn

Name	Mutation	Oligonucleotides ^a
L137E	Leu137 to Glu	5'-TGG CCC GAG GCC <u>GAGGCT</u> ATC AGT CAG-3' 5'-CTG ACT GAT AGC <u>CTC</u> GGC CTC GGG CCA-3'
D132E/L137E	Leu137 to Glu Asp132 to Glu	5'-TGG GGT GGG <u>GAA</u> TGG CCC GAG GCC GAG-3' 5'-CTC GGC CTC GGG CCA <u>TTC</u> CCC ACC CCA-3'
L137E/loop121–132	Leu137 to Glu plus human 121–132 to mouse 121–132	5'- <u>CCA</u> AGG ATT GGC AAC TGG ACT GGA GAA TGG CCC GAG GCC-3' 5'-A <u>GTT</u> GCC AAT CCT TGG GTT GAA TTT CAT GAA CTC CTC GCC-3'
L137E/loop79–89	Leu 137 to Glu plus human 79–89 to mouse 79–89	5'-TTG GAA AAG ATT CTA AAT GGT ACC TAC ACT CTG CAG GGC CTG-3' 5'-ATT TAG AAT CTT TTC CAA AGT TTT TAA AGC TTC CAG AAA-3'

^a Mutated codons are indicated by underlining.

Asp137 (FcRn) contacts His436 (IgG) (Figure 2). His436 is replaced by Tyr or Phe in human IgG,³⁵ leading to the suggestion that the Asp137–His436 interaction for rat FcRn might be replaced by Leu137–Tyr/Phe436 in the human FcRn–IgG complex.²⁹ In mouse FcRn, Asp137 of rat FcRn is replaced by Glu137,³³ and Leu137 of human FcRn was therefore mutated to Glu137.

Significant differences between human and mouse FcRn that might be relevant to IgG binding also lie in the region encompassing residues 121–132 (Figures 1 and 2).^{18,33} This region has been mutated en bloc to the corresponding mouse sequence in combination with the L137E mutation to generate the L137E/loop121–132 mutant. This loop includes Asp132 (human), which has been replaced by Glu132 (mouse) either in the en bloc mutation or as a double mutation in combination with L137E (D132E/L137E). In addition, complex-type carbohydrate attached to an N-linked glycosylation site at residue 128 that is present in rat/mouse FcRn but not in human FcRn has been

shown to contact Val348, His433, Asn434 and Lys439 of Fc in the crystal complex of rat FcRn bound to rat Fc.²⁹ However, mutation of His433 or Asn434 of mouse Fc to alanine does not affect the activity of the Fc fragment in mouse FcRn-mediated functions,²⁷ despite the fact that mouse FcRn is highly homologous to rat FcRn and has the same potential glycosylation sites. This suggests that the complex carbohydrate–IgG interactions may not be functionally relevant, at least for the mouse FcRn–mouse IgG1 complex. In this context, although it has been shown that for a subset of FcRn–Fc interactions the presence of complex carbohydrate *versus* high-mannose forms of carbohydrate can affect binding,³⁶ this cannot be used to explain the differential binding of human and mouse FcRn to mouse IgG isotypes, as both FcRn species were expressed in insect cells (Ober *et al.*,²⁴ this study).

A further obvious difference between human and mouse FcRn is that the former has a two amino acid deletion of residues 85 and 86 in the $\alpha 1$ domain,¹⁸ and residues 79–89, which flank this region, are also distinct (Figure 1). This deletion removes a bulge in the vicinity of the FcRn–IgG interaction site,³⁷ and residues 86 (Ile) and 90 (Phe) of rat FcRn have been shown to contact rat Fc residue 254 (Figure 2).²⁹ These two FcRn residues are replaced conservatively by Leu86 and Tyr90 in mouse FcRn (Figure 1; Table 2). In addition rodent, but not human, FcRn has a potential N-linked glycosylation site at position 87. The attached sugar molecule does not contact Fc in the rat Fc–FcRn complex,²⁹ but it is possible that this bulky moiety could affect the disposition of Fc on FcRn. The effect of replacing human FcRn residues 79–89 with the corresponding mouse FcRn sequences has therefore been investigated in the current study.

Wild-type and mutated variants of human FcRn were purified from baculovirus-infected High-5 cells. All mutants were purified using Ni²⁺-NTA-agarose followed by size-exclusion chromatography to exclude aggregates. A representative size-exclusion (Superdex 200) chromatography trace of one of the mutants is shown in Figure 3,

Table 2. Residues predicted to be involved in FcRn–IgG interactions

Human FcRn	Human IgG	Mouse FcRn	Mouse IgG1,IgG2a	Mouse IgG2b
Deleted^a	Ser254	Leu86^b	Thr254^c	Ser254
Tyr90	Ser254	Tyr90	Thr254	Ser254
Glu117	His310	Glu117	His310	His310
Glu118	Gln311	Glu118	Gln311	Gln311
Asp132	His435^d	Glu132	His435	Tyr435
Trp133	Ile253	Trp133	Ile253	Ile253
Leu137	Tyr436^e	Glu137	His436	Tyr436

Residues are predicted from the X-ray crystallographic structure of rat FcRn complexed with rat IgG2a derived Fc.²⁹ Note that for human FcRn the two amino acid deletion (residues 85 and 86) is ignored in the numbering, which corresponds to the homology alignment of rodent and human FcRn.^{18,33,34}

^a Residues 85 and 86 of human FcRn are deleted.

^b Sequence differences are indicated in bold.

^c In mouse IgG2a, residue 254 is Ser.³⁵

^d In all human isotypes, except in an IgG3 allotype, where residue 435 is Arg.³⁵

^e In all human isotypes, except in an IgG3 allotype, where residue 436 is Phe.³⁵

rFcRn	1	<u>A</u> SPRLP <u>LM</u> YHLAAVSDLSTGLPSFWATGWLGA <u>QO</u> YLYNNLRQ <u>EA</u> DPGAWI <u>W</u> ENQVSWY 60
mFcRn	1	S <u>E</u> TRPP <u>LM</u> YHLTAVSNPSTGLPSFWATGWL <u>G</u> P <u>QO</u> YLYNNLRQ <u>EA</u> DPGAWI <u>W</u> ENQVSWY 60
hFcRn	1	A <u>S</u> SHLS <u>LL</u> YHLTAVSSPAPGTPAFWVSGWL <u>G</u> P <u>QO</u> YLYNNLRQ <u>EA</u> DPGAWI <u>W</u> ENQVSWY 60
rFcRn	61	WEKET <u>TD</u> LKSK <u>EQ</u> LFLEAIR <u>TE</u> ENQIN <u>GT</u> FTLQGLLGCELAP <u>DN</u> SS <u>LP</u> TAVFALNGEEFM 120
mFcRn	61	WEKET <u>TD</u> LKSK <u>EQ</u> LFLEALK <u>TE</u> EKILN <u>GT</u> TYTLQGLLGCELAS <u>DN</u> SS <u>LP</u> TAVFALNGEEFM 120
hFcRn	61	WEKET <u>TD</u> LRIK <u>EQ</u> LFLEAFKALGG--K <u>GP</u> YTLQGLLGCEL <u>GD</u> NT <u>SV</u> PTARFALNGEEFM 120
rFcRn	121	R <u>EN</u> PRIC <u>N</u> WS <u>GE</u> WPETDIVGNLW <u>MK</u> PEA <u>AR</u> KESE <u>FL</u> LTSC <u>PE</u> RL <u>LGH</u> L <u>ERGR</u> ONLEWKE 180
mFcRn	121	R <u>EN</u> PRIC <u>N</u> WT <u>GE</u> WPETDIVANLW <u>MK</u> PD <u>AA</u> RK <u>ES</u> EFLLNS <u>CP</u> ER <u>LGH</u> L <u>ERGR</u> RRNLEWKE 180
hFcRn	121	N <u>ED</u> LK <u>Q</u> CTW <u>GE</u> WP <u>EA</u> L <u>AI</u> SQRW <u>Q</u> Q <u>DK</u> A <u>AN</u> KELT <u>FL</u> LFSC <u>PH</u> RL <u>RE</u> H <u>L</u> ERGRGNLEWKE 180
rFcRn	181	PPSMRLK <u>AR</u> PGNS <u>GS</u> SVLTC <u>AA</u> FSFY <u>PE</u> ELK <u>FR</u> FLR <u>NG</u> LAS <u>GS</u> GN <u>CS</u> T <u>GP</u> NG <u>DG</u> S <u>FH</u> AW <u>S</u> 240
mFcRn	181	PPSMRLK <u>AR</u> PGNS <u>GS</u> SVLTC <u>AA</u> FSFY <u>PE</u> ELK <u>FR</u> FLR <u>NG</u> LAS <u>GS</u> GN <u>CS</u> T <u>GP</u> NG <u>DG</u> S <u>FH</u> AW <u>S</u> 240
hFcRn	181	PPSMRLK <u>AR</u> PS <u>SF</u> GF <u>SV</u> LTC <u>SA</u> FSFY <u>PE</u> EL <u>QR</u> FLR <u>NG</u> LAA <u>CT</u> CG <u>DF</u> GP <u>NS</u> D <u>GS</u> F <u>H</u> AW <u>S</u> 240
rFcRn	241	L <u>LE</u> VKR <u>G</u> DE <u>HH</u> Y <u>QC</u> Q <u>VE</u> BE <u>GL</u> AQ <u>PL</u> IV <u>DL</u> DS <u>PA</u> R <u>SS</u> V <u>P</u> V <u>VG</u> I <u>IL</u> GL <u>LL</u> V <u>V</u> V <u>AI</u> AG <u>V</u> LLW 300
mFcRn	241	L <u>LE</u> VKR <u>G</u> DE <u>HH</u> Y <u>QC</u> Q <u>VE</u> BE <u>GL</u> AQ <u>PL</u> IV <u>DL</u> DS <u>SA</u> R <u>SS</u> V <u>P</u> V <u>VG</u> I <u>IV</u> LG <u>LL</u> V <u>V</u> V <u>AI</u> AG <u>V</u> LLW 300
hFcRn	241	S <u>LE</u> V <u>K</u> S <u>G</u> DE <u>HH</u> Y <u>CC</u> I <u>V</u> Q <u>H</u> AG <u>LA</u> Q <u>PL</u> R <u>VE</u> LE <u>SP</u> A <u>K</u> SS <u>V</u> L <u>V</u> V <u>GI</u> V <u>IG</u> V <u>LL</u> LT <u>AA</u> AV <u>GC</u> ALLW 300
rFcRn	301	R <u>MR</u> SG <u>L</u> P <u>AP</u> W <u>LS</u> LS <u>G</u> DD <u>SG</u> DL <u>LP</u> GG <u>N</u> LP <u>PE</u> AE <u>PQ</u> GV <u>NA</u> FP <u>ATS</u> * 345
mFcRn	301	R <u>MR</u> SG <u>L</u> P <u>AP</u> W <u>LS</u> LS <u>G</u> DD <u>SG</u> DL <u>LP</u> GG <u>N</u> LP <u>PE</u> AE <u>PQ</u> GA <u>NA</u> FP <u>ATS</u> * 345
hFcRn	301	R <u>MR</u> SG <u>L</u> P <u>AP</u> W <u>LS</u> LR <u>G</u> DD <u>IG</u> V <u>LL</u> PT <u>PG</u> EA <u>Q</u> DA <u>LD</u> K <u>D</u> V <u>NV</u> I <u>P</u> A <u>T</u> A* 345

Figure 1. Sequence alignment of rat,³⁴ mouse³³ and human FcRn¹⁸ with identical sequences indicated by shading. Potential N-linked glycosylation sites at positions 87, 128, 225 (present in mouse and rat FcRn) and 104 (present in all three FcRn species) are indicated by underlining.

and indicates that the major component of the FcRn preparation before purification is not aggregated i.e. FcRn α -chain: β 2-microglobulin (β 2m) heterodimers of \sim 60 kDa. The peak that elutes between fractions 1 and 10 corresponds to a molecular mass of about 120 kDa and is therefore most likely dimers of FcRn. Similar traces were seen for all other wild-type and mutated FcRn forms (data not shown). These proteins were analyzed for binding to human IgG1 and mouse IgGs using SPR. For comparative purposes, the binding of mouse FcRn to these IgGs was analyzed. As the IgG–FcRn interaction involves two possible binding sites on IgG that may not be equivalent,^{36,38} all equilibrium binding (dissociation) constants should be taken as apparent constants. However, they represent good estimates of the relative affinities of the interactions. Under the conditions of the

experiments, the major contribution to binding, at least for the mouse interaction where the affinities of the two sites have been determined by sedimentation equilibrium,³⁸ comes from the higher-affinity site. In all cases, affinities were determined with immobilized IgG, rather than FcRn, to avoid avidity effects.

We have recently described an analytical method for determining equilibrium binding constants by SPR in which the loss of activity of ligand on the sensor chip during the course of the experiment is taken into account.³⁹ This method, which involves the use of multiple analyte injections over a prolonged period of time, was employed for the higher-affinity interactions ($K_D < 2 \mu\text{M}$) and resulted in dissociation constants similar to those obtained by Scatchard analyses (shown in Figure 4 for the interaction of mouse FcRn with mouse

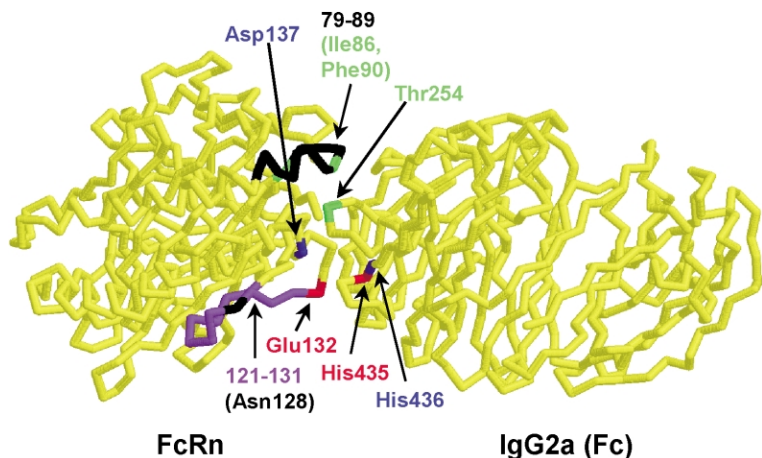


Figure 2. The α carbon trace of the rat FcRn–rat IgG2a (Fc) structure²⁹ with location of FcRn residues that have been used to replace the corresponding human FcRn sequence in the current study indicated. Glu132 (red) and Asp137 (blue) interact with His435 (red) and His436 (blue), respectively, of IgG. Ile86 and Phe90 (green) of rat FcRn, contained within the residue 79–89 mutation, also make contact with Thr254 (green) of rat Fc. Although residues 121–131 (purple), with the N-linked glycosylation site at Asn128 indicated in black) do not contact Fc directly, this region is not conserved and has been mutated. The carbohydrate attached to Asn128 also contacts Fc,²⁹ and, for clarity, is not shown.

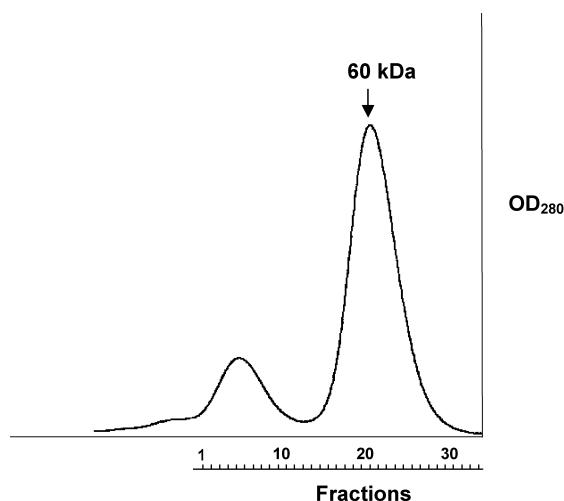


Figure 3. Gel-filtration chromatography of human FcRn (L137E mutant) using a HiLoad™ 26/60 Superdex™ 200 preparation grade column to purify FcRn (60 kDa). As a first step of purification, affinity chromatography using Ni²⁺-NTA-agarose was carried out.

IgG1). It became apparent from initial analyses that lower affinity interactions ($K_D > 5 \mu\text{M}$) required the use of relatively high concentrations of analyte (up to $33 \mu\text{M}$, or 2 mg/ml) to obtain reliable data. Due to limitations in the amounts of recombinant protein, these interactions were analyzed using lower numbers of analyte injections, which precluded the use of our analytical method. K_D values for these interactions were therefore determined by Scatchard analyses.

The L137E mutation generates a human FcRn variant that binds to mouse IgG1

Mutation of Leu137 to Glu (L137E) in human FcRn results in a variant that binds to mouse IgG1 with a dissociation constant of $13.2 \mu\text{M}$ (Table 3; Figure 5). Consistent with earlier data, wild-type human FcRn shows very weak binding to mouse IgG1, for which the dissociation constant cannot be determined accurately by Scatchard analyses due to the extremely high concentrations of analyte that would be required (Figure 5). The dissociation constant of the L137E mutant for human IgG1 is increased by about twofold from $0.63 \mu\text{M}$ (wild-type) to $1.7 \mu\text{M}$ (Table 3). Conversion of Leu137 to Glu therefore results in a substantial improvement in the binding of human FcRn to mouse IgG1. However, as the dissociation constant of $13.2 \mu\text{M}$ is about 18-fold greater than that of the mouse FcRn–mouse IgG1 interaction ($0.75 \mu\text{M}$), we attempted to increase the affinity of the L137E–mouse IgG1 complex further by additional rounds of mutagenesis of residues in the vicinity of the L137E mutation. (1) The combination of both D132E and L137E mutations results in a human FcRn variant with properties similar to those of the L137E mutant (data not shown). (2) The replacement of residues 121–132 in combination with L137E (L137E/loop121–132) results in an approximately twofold increase in dissociation constants for the corresponding interactions with human and mouse IgG1 (Table 3). (3) The replacement of residues 79–89 with the corresponding region of mouse FcRn to generate the L137E/loop79–89

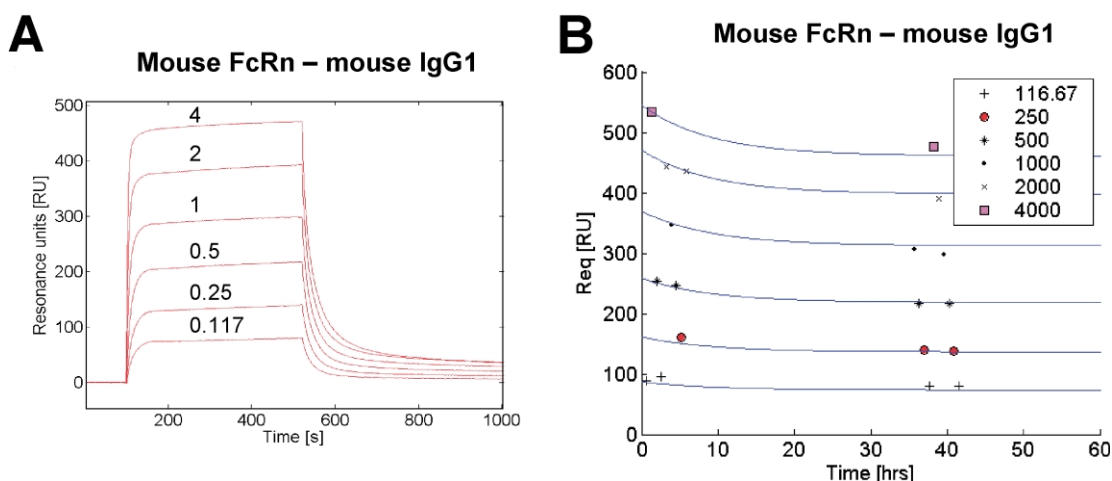


Figure 4. SPR analyses of the interaction of mouse FcRn with mouse IgG1 using an analytical method³⁹ to account for loss of ligand activity during the course of the experiment. Different concentrations of FcRn (0.117– $4 \mu\text{M}$) were injected over a flow-cell coupled with mouse IgG1 (1466 resonance units) in PBS (pH 6.0), 0.01% Tween, at a flow-rate of $10 \mu\text{l/minute}$. (A) Sensorgrams corresponding to each concentration (in μM) of mouse FcRn used. Data from injections performed at about 38–42 hours are plotted. All sensorgrams were zero adjusted and reference cell data subtracted. (B) Data were analyzed using the method described by Ober & Ward.³⁹ This method involves two “blocks” of injections over an extended period of time, and each data point shown represents the signal level (RU) corresponding to an analyte injection (concentration indicated in nM) at the time indicated after the start of the experiment. To obtain the dissociation constant of $0.75 \mu\text{M}$, data were fit to the analytical equations described by Ober & Ward.³⁹ Scatchard analyses of the same data resulted in a dissociation constant estimate of $0.7 \mu\text{M}$. Concentrations are indicated in B in nM.

Table 3. Equilibrium dissociation constants (K_D) of wild-type human/mouse FcRn and mutated human FcRn variants for IgGs at pH 6.0

FcRn type	K_D (μM)			
	Human IgG1	Mouse IgG1	Mouse IgG2a	Mouse IgG2b
Wild-type human	0.63	WB	WB	18.1
Wild-type mouse	0.082	0.75	0.42	0.5
L137E	1.7	13.2	14.4	11.7
L137E/loop121–132	3.5	25.7	14.2	17.8
L137E/loop79–89	1.4	28.2	15.7	5.2
Loop79–89	0.55	WB	WB	5.2

WB, very weak binding with $K_D > 50 \mu\text{M}$.

mutant results in a loss in affinity (dissociation constants of $13.2 \mu\text{M}$ for L137E *versus* $28.2 \mu\text{M}$ for L137E/loop79–89) for binding to mouse IgG1 (Table 3). In addition, the binding of this mutant

to human IgG1 is similar to that of the L137E mutant, with a dissociation constant that is about twofold higher than that of the parent wild-type FcRn (Table 3).

For several of the mutants (L137E, L137E/loop79–89), we assessed the effect of substitution of human $\beta 2\text{m}$ by mouse $\beta 2\text{m}$ to exclude the possibility that this could account for the differences in cross-species binding. This results in insignificant differences in binding affinities (data not shown), and is consistent with the identity of residues 1 and 2 of $\beta 2\text{m}$, which, in the rat FcRn–rat Fc complex, make contact with Fc ligand.²⁹

Interaction of the mutants with mouse IgG2a and IgG2b

We next analyzed the binding of the mutated FcRn molecules to mouse IgG2a and IgG2b. Mouse IgG1 and IgG2a have histidine at positions 435 and 436, whereas mouse IgG2b has tyrosine at these two positions (Table 2). As human IgG1 has tyrosine at position 436, it was therefore of interest

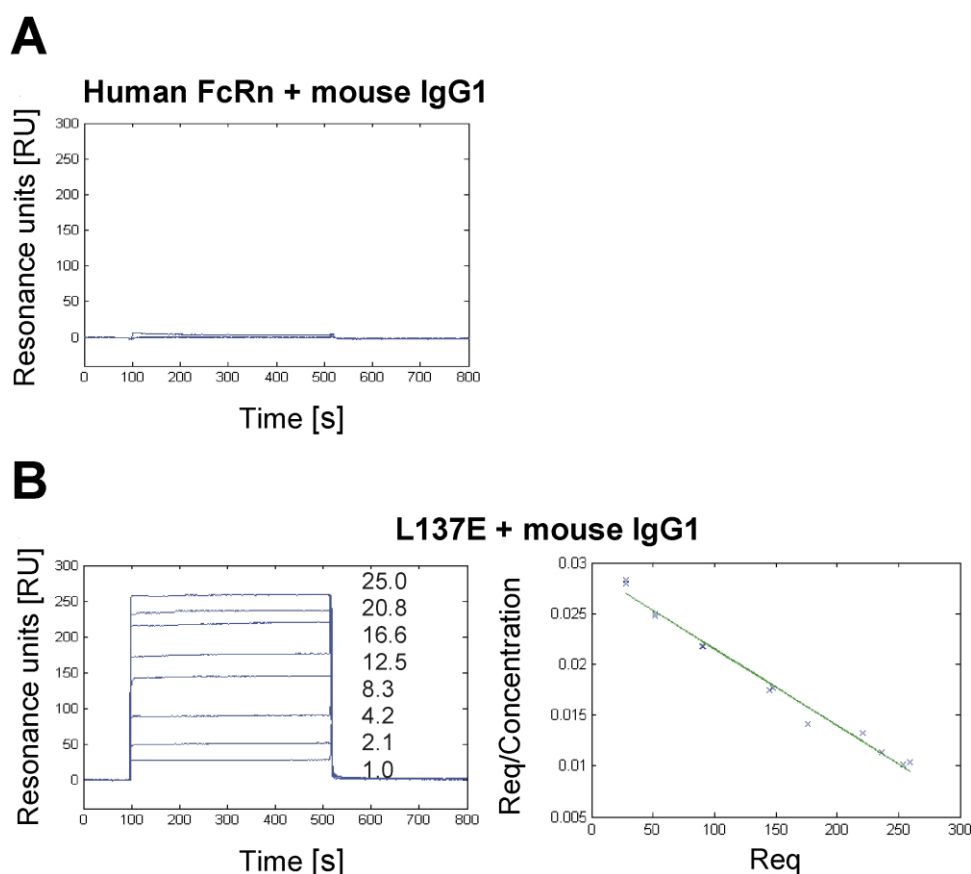


Figure 5. SPR analyses of the interactions of wild-type human FcRn (A) and L137E mutant (B) with mouse IgG1. The coupling density of mouse IgG1 was 1042 resonance units. Different concentrations of FcRn ($0.25\text{--}2 \mu\text{M}$ for wild-type, $1\text{--}25 \mu\text{M}$ for L137E) were injected over the flow-cells in PBS (pH 6.0), 0.01% Tween, at a flow-rate of $10 \mu\text{l}/\text{minute}$. (Higher concentrations of wild-type human FcRn were not used as a binding signal of only four resonance units was seen when used at a concentration of $2 \mu\text{M}$). For most concentrations, duplicate injections were carried out and representative sensorgrams for each duplicate are plotted. Concentrations of L137E (in μM) corresponding to each sensorgram are shown. All sensorgrams were zero adjusted and reference cell data (flow-cell coupled with buffer only during the coupling cycle) subtracted. The Scatchard plot was generated using concentrations in nM.

to compare the binding of the different mouse IgG subtypes to the mutated FcRn variants. In a previous study, we have shown that human FcRn binds to mouse IgG2a with a dissociation constant that was too high to be determined accurately by Scatchard analyses, whereas weak binding to mouse IgG2b can be detected.²⁴ Here, by using higher concentrations of analyte than were used by Ober *et al.*,²⁴ we have determined the dissociation constant of the human FcRn–mouse IgG2b interaction to be 18.1 μM (Table 3). The L137E mutant binds to mouse IgG2a and mouse IgG2b with dissociation constants that are essentially the same as those of the interaction of this mutant with mouse IgG1 (Table 3; Figure 6), and similar affinities were obtained for the D132E/L137E mutant (data not shown). Comparison of the interactions of the L137E mutant for these mouse IgG subtypes indicate that, although this FcRn variant has acquired significant binding activity, the dissociation constants are again higher than for the corresponding mouse FcRn–mouse IgG interactions (Table 3). Relative to the effect of the L137E mutation, the combination of the loop121–132 mutation with L137E resulted in either a slight increase (mouse IgG2b) or no change (mouse IgG2a) in dissociation constant. The effects of combining the L137E and loop79–89 mutations (L137E/loop79–89) were unexpected: this mutant binds to mouse IgG2a with a dissociation constant that is similar to that of the L137E–mouse IgG2a interaction, whereas the dissociation constant for mouse IgG2b is lower (5.2 μM versus 11.7 μM) (Table 3; Figure 6).

To further investigate the effects of the loop79–89 mutation, a variant with this mutation in the absence of L137E was analyzed. This mutant (loop79–89) has the same dissociation constant as the L137E/loop79–89 mutant for binding to mouse IgG2b, whereas the dissociation constant for human IgG1 is close to that of the wild-type human FcRn–human IgG1 interaction (0.55 μM versus 0.63 μM ; Table 3). This mutant also resembles the wild-type human FcRn, as it binds to both mouse IgG1 and IgG2a very poorly (Table 3).

Effects of the mutations on the pH-dependence of the FcRn–IgG interactions

The pH-dependence (higher-affinity binding at pH 6.0–6.5 relative to pH 7.3⁴⁰) of the FcRn–IgG interaction is believed to be important for FcRn to carry out its role as an IgG transporter.¹⁷ The interactions of the wild-type and mutated FcRn molecules with human and mouse IgGs at pH 7.3 were therefore analyzed. Sensorgrams for binding of the L137E mutant to mouse/human IgGs at pH 6.0 and 7.3 are shown in Figure 7. Similar behavior was observed for wild-type human FcRn and all other mutated FcRn species (data not shown). However, the binding of wild-type human FcRn to human IgG1 showed slightly less pH-dependence than the interactions of the FcRn mutants with

this IgG (Figure 7(D) and (E); and data not shown). In addition, the pH-dependencies of the interactions of all FcRn species (including mouse FcRn) with mouse IgG2b are less marked than those for other mouse IgGs (Figure 7, data not shown). This is consistent with earlier studies of the rat FcRn–mouse IgG2b interaction.⁴⁰ In all cases, the poor binding at pH 7.3 precluded accurate determination of equilibrium dissociation constants by Scatchard analyses. In qualitative terms, however, the mutated FcRn molecules retain pH-dependencies for the corresponding interactions with ligand similar to that of wild-type human FcRn.

Discussion

In the current study we have investigated the molecular basis for the difference in binding specificity between human and mouse FcRn. We previously reported that human FcRn does not bind detectably to mouse IgG1 or IgG2a, and has a low affinity for mouse IgG2b.²⁴ As FcRn is a protective receptor that regulates serum IgG levels, this observation provides an explanation for the long misunderstood phenomenon that mouse IgG1 has a short serum half-life in humans.^{31,32} Detailed knowledge as to why human FcRn does not bind to mouse IgG1/IgG2a has relevance to understanding the molecular basis of FcRn–IgG interactions in humans. As this receptor is involved in regulating IgG levels at diverse body sites, including in the serum, such analyses are of importance to understanding the factors that control the humoral immune response.

Human and mouse FcRn share a high degree of homology, and the FcRn residues that are involved in binding to IgG are generally well conserved (Figure 1; Table 2).⁴¹ However, there are several differences: first, Leu137 (human) is replaced by Glu (mouse); second, Asp132 (human) is replaced by Glu (mouse); third, there is a two residue deletion (residues 85 and 86) in the $\alpha 1$ domain of human FcRn. Residues 79–89 surrounding this region are distinct, and in rodent FcRn include an N-linked glycosylation site (Asn87); fourth, amino acid residues in a loop encompassing residues 121–132 are not well conserved, and Asn128 of rodent FcRn is a potential site for N-linked glycosylation. With the aim of transferring the binding properties of mouse FcRn to human FcRn, we systematically mutated human FcRn to replace regions or residues by the corresponding murine residues. Recombinant mutated human FcRn proteins were purified and analyzed for binding to human IgG1 and mouse IgG1, IgG2a, IgG2b using SPR.

Mutation of Leu137 to Glu resulted in a human FcRn variant that binds to mouse IgG1, IgG2a and IgG2b with similar dissociation constants (11.7–14.4 μM). The L137E mutant shows an approximate twofold increase (0.63 versus 1.7 μM) in dissociation constant for human IgG1. Despite the

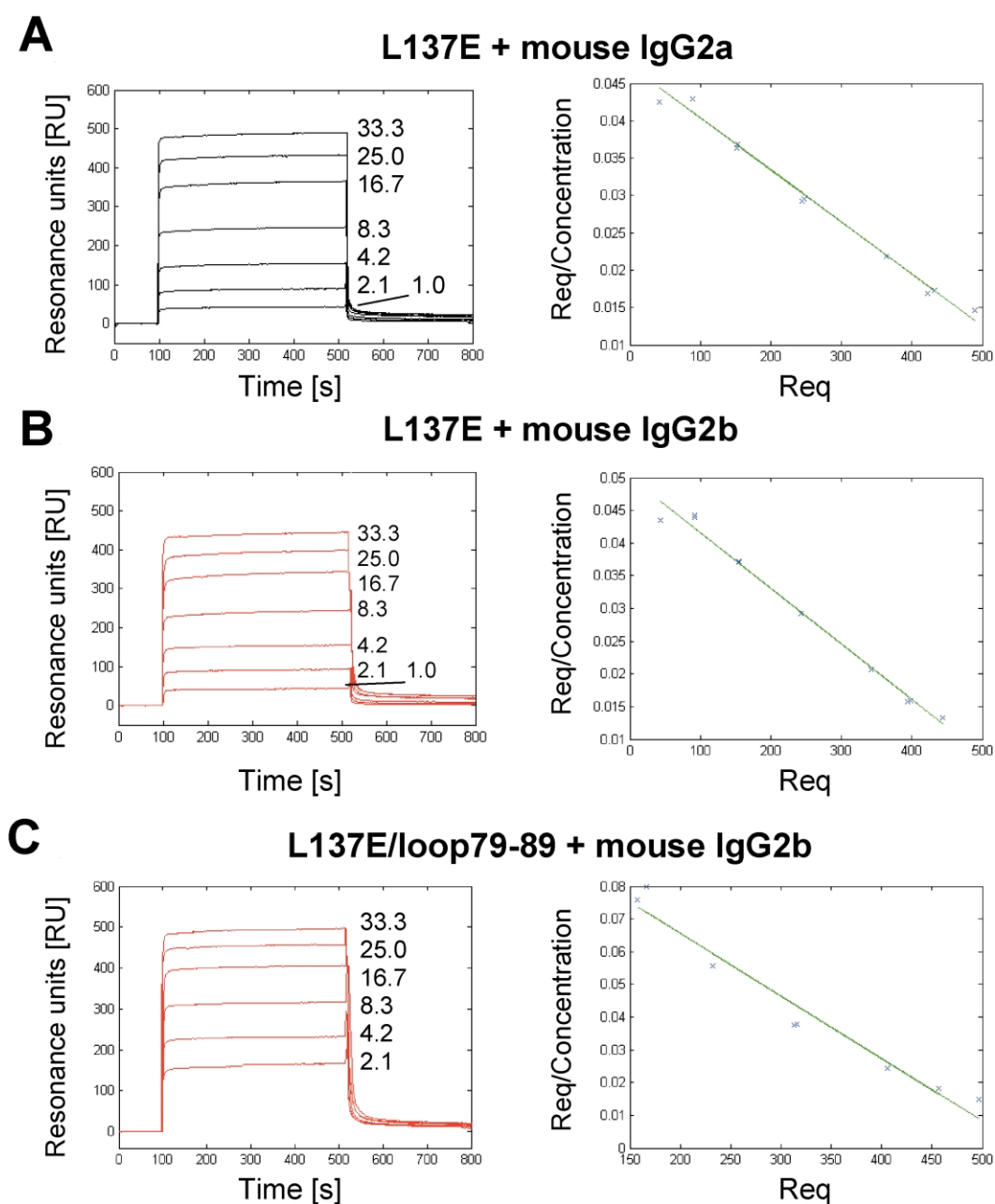


Figure 6. SPR analyses of the interactions of (A) L137E mutant with mouse IgG2a; (B) L137E mutant with mouse IgG2b; (C) L137E/loop79–89 mutant with mouse IgG2b. The coupling densities were 1278 resonance units for mouse IgG2a and 1013 resonance units for mouse IgG2b. Different concentrations of FcRn (1–33.3 μM) were injected over the flow-cells in PBS (pH 6.0), 0.01% Tween, at a flow-rate of 10 $\mu\text{l}/\text{minute}$. For most concentrations, duplicate injections were carried out and representative sensorgrams for each duplicate are plotted. Concentrations of mutated FcRn (in μM) corresponding to each sensorgram are shown. All sensorgrams were zero adjusted and reference cell data (flow-cell coupled with buffer only during the coupling cycle) subtracted. The Scatchard plots were generated using concentrations in nM.

ability of the L137E mutation to convert human FcRn into a form that binds to mouse IgGs, it is apparent that the dissociation constants for the L137E mutant for mouse IgGs are all significantly higher than those of the corresponding mouse FcRn–mouse IgG interactions. In an attempt to further increase the affinities of human FcRn for these IgGs, additional mutations were therefore superimposed on the L137E mutant. Mutation of

Asp132 to Glu (D132E) does not significantly affect the binding properties. Replacement of residues 121–132 of human FcRn with the corresponding sequence of mouse FcRn results in reductions in binding affinity for three of the four IgGs analyzed, indicating that this mutation induces conformational effects that are detrimental to complex formation. Finally, the insertion of residues 85 and 86, together with mutation of the flanking residues

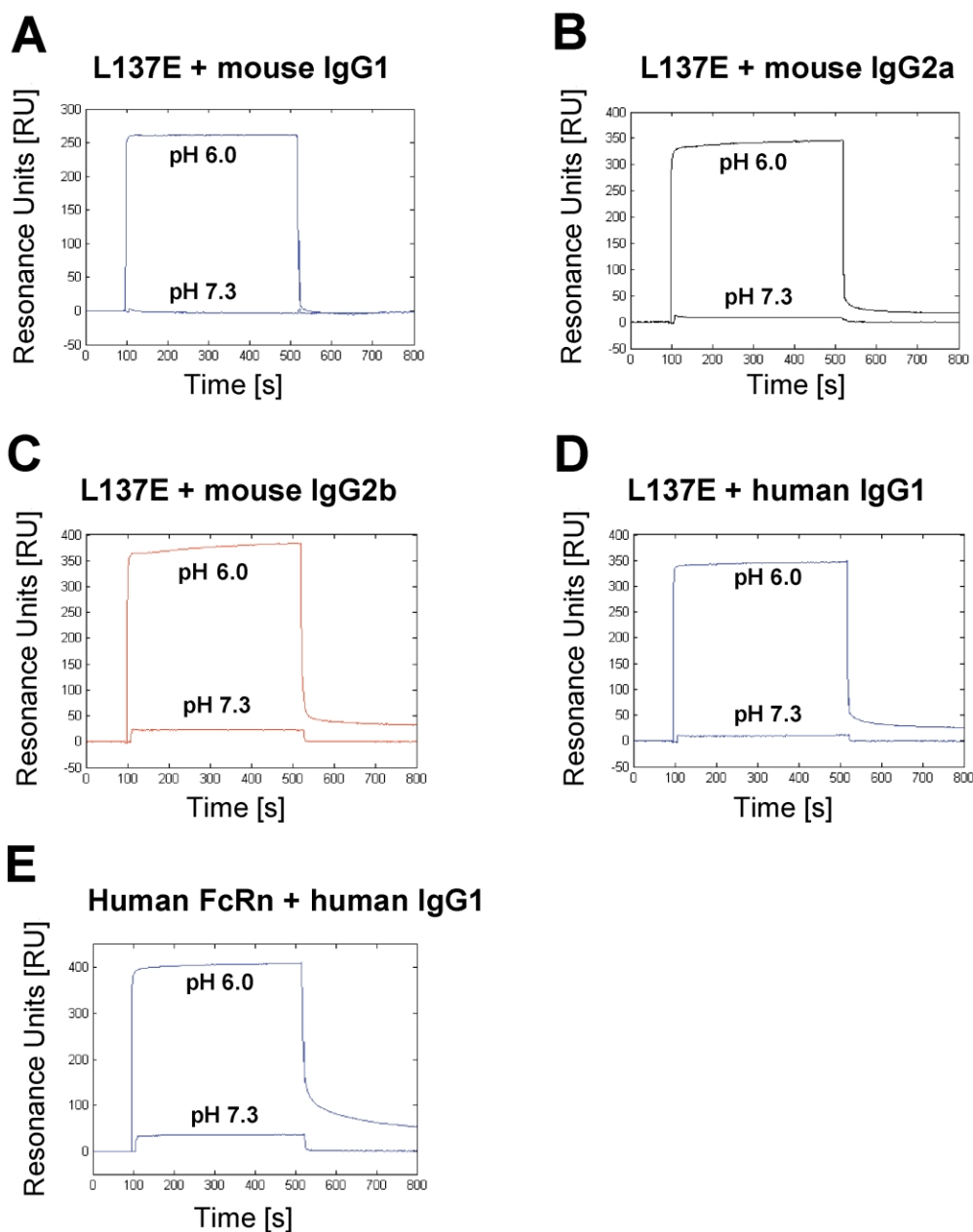


Figure 7. The pH-dependence of the interactions of (A) L137E mutant with mouse IgG1 (1367 resonance units coupled); (B) L137E mutant with mouse IgG2a (1209 resonance units coupled); (C) L137E mutant with mouse IgG2b (1119 resonance units coupled); (D) L137E mutant with human IgG1 (678 resonance units coupled); (E) wild-type human FcRn with human IgG1 (678 resonance units coupled). PBS (pH 6.0 or 7.3 as indicated), 0.01% Tween, was used as running buffer. Sensorgrams for 16.7 μ M L137E mutant (A)–(D) or wild-type FcRn (E) at each pH value are shown, and are representative of duplicate injections. All sensorgrams were zero adjusted and reference cell data (flow-cell coupled with buffer only during the coupling cycle) subtracted.

(79–89) in this region, has unexpected results: relative to the L137E mutant, the L137E/loop79–89 mutant has an approximately twofold decreased dissociation constant for mouse IgG2b, whereas the dissociation constant for mouse IgG1 is increased about twofold. We do not have an explanation at the molecular level for these effects.

The question arises as to what is the molecular basis of the effects of the mutations? In the rat FcRn–rat Fc interaction, Asp137 interacts with His436, leading to the earlier suggestion that for

human FcRn, Leu137 might interact with Tyr436 of human IgG1.²⁹ Although the supposition that this interaction occurs can be used to explain some of our results, it cannot be applied generally. On the basis of the data, we can divide the FcRn species in this study into two classes: mouse FcRn-like (wild-type mouse FcRn, L137E, D132E/L137E and L137E/loop121–132) and human FcRn-like (wild-type human FcRn, L137E /loop79–89, loop79–89). For an individual FcRn species within the mouse FcRn-like class, binding to all mouse IgG subtypes

with similar dissociation constants is observed (Table 3). In contrast, human FcRn-like molecules discriminate between these IgGs. Significantly, a single mutation (L137E) can convert human FcRn into a member of the mouse FcRn-like class. Unexpectedly, the affinity of the interactions of most mouse FcRn-like molecules (all containing Glu137) with mouse IgGs does not appear to be affected negatively by the substitution of histidine (mouse IgG1, IgG2a) at position 436 by tyrosine (mouse IgG2b). For example, the dissociation constant of mouse FcRn for mouse IgG2b is slightly lower than that for the interaction with mouse IgG1, and the L137E (human FcRn) variant has a similar dissociation constant for both mouse IgG1 and IgG2b. Thus, in one case an affinity improvement is seen when the apparently favorable Glu137 (FcRn)–His436 (IgG) interaction is replaced by Glu137–Tyr436. This suggests that for Tyr436-containing IgGs such as mouse IgG2b, less favorable Glu137–Tyr436 interactions may be compensated for by other stabilizing effects. For example, IgG2b has tyrosine rather than histidine at position 435, and it is tempting to suggest that this may enhance the binding affinity through hydrophobic interactions with Trp133 of FcRn whilst decreasing the pH-dependence of the FcRn–IgG interaction (Raghavan *et al.*;⁴⁰ and our unpublished observations). Clearly, however, in the absence of high-resolution structural data, it is not possible to predict the nature of the IgG Tyr436–FcRn interaction.

In contrast to the indications that the FcRn–mouse IgG2b interactions are insensitive to variations at residue 137 of FcRn, all mutants containing L137E consistently have at least a twofold increase in dissociation constant for binding to human IgG1. This suggests that the contribution of the interaction of IgG residue 436 with FcRn residue 137 might be variable for different IgG species. In turn, this might be a consequence of variability in the topology of the interaction. In this context, in two independent studies, mutation of residue 436 of human or mouse IgG1 to alanine was shown to result in a loss of binding activity for human or mouse FcRn, respectively.^{27,42} This loss of activity is consistent with our current data demonstrating that the IgG residue 436–FcRn residue 137 pair is involved in the human FcRn–human IgG1 interaction, although the only twofold reduction in affinity seen in our studies suggest that it is not central to binding. However, based on our observations here it is likely that the effects of mutation of IgG residue 436 on FcRn-mediated functions will vary across species and isotypes.

In contrast to mouse FcRn-like proteins, those of the human FcRn-like class bind less well to His436-containing IgGs (mouse IgG1 and IgG2a) relative to Tyr436-containing IgGs (mouse IgG2b, human IgG1). Wild-type human FcRn and the loop79–89 mutant are extreme cases of this class for which the dissociation constants for IgGs with His436 are immeasurably high, in contrast to

those for IgGs with Tyr436 (Table 3). Unexpectedly, the L137E/loop79–89 mutant also falls into this class, despite the presence of glutamic acid at position 137 which would be predicted to interact favorably with His436. Thus, when in the context of human FcRn containing Glu137, residues 79–89 of mouse FcRn appear to modulate the docking of FcRn on IgG so that it binds to mouse IgG2b with a dissociation constant that is about three- to five-fold lower than that for binding to mouse IgG2a and IgG1. In addition, the L137E/loop79–89 mutant shows significantly better binding to mouse IgG2b relative to the parent wild-type FcRn. By comparing the L137E/loop79–89 and loop79–89 mutants, we again do not see an impact of the compatibility of mouse IgG2b residue 436–FcRn residue 137 on binding, indicating that this may be a general feature for all interactions involving this mouse IgG. In contrast, the lower dissociation constant of the loop79–89 mutant relative to the L137E/loop79–89 mutant for binding to human IgG1 further reinforces the requirement for Leu137 for optimal binding to human IgG1 by human FcRn and its mutated derivatives.

It is noticeable that the binding to human IgG1 of all FcRn species analyzed in this study are of higher affinity than the corresponding FcRn–mouse IgG interactions. This higher affinity for human IgG1 is seen even for mouse FcRn, and strengthens the concept that there may be differences in overall configuration of the FcRn–IgG interaction across species. Nevertheless, it is interesting that the dissociation constants of the homologous (i.e. mouse–mouse, human–human) interactions fall in a similar range ($\sim 0.5 \mu\text{M}$), suggesting that each FcRn species has evolved to have an affinity for homologous IgG that is optimal for IgG homeostasis and transport.

Although we have shown that it is possible to confer binding of mouse IgGs on human FcRn by mutagenesis of selected residues, the dissociation constants of the human FcRn variants are generally at least ~ 18 -fold higher than those of the corresponding mouse FcRn interactions. Further, the dissociation constant of the human IgG1–human FcRn interaction is also about eightfold higher than the heterologous human IgG1–mouse FcRn interaction (Table 3).²² Thus, relative to human FcRn, for a given IgG, mouse FcRn binds more strongly. Although it has been proposed that additional carbohydrate on mouse/rat FcRn may be responsible for the higher affinity,²⁹ the form of carbohydrate present on insect cell-expressed FcRn is of an immature type,⁴³ rather than the complex type that was present in the crystallized rat FcRn–Fc complex.²⁹ This makes it less likely that the high-mannose carbohydrate makes significant contributions to binding in the current study. Furthermore, the role of complex carbohydrate at position 128 of mouse FcRn in binding to mouse IgG1 is questionable, since mutation of two of the presumptive Fc/IgG contact residues, His433 and Asn434, does not affect the corresponding

FcRn–Fc interaction.²⁷ An alternative explanation for the higher affinity of the interaction of mouse FcRn with IgGs is that Trp133 of FcRn, which makes hydrophobic interactions with Ile253,²⁹ is more exposed in rodent (rat) FcRn relative to human FcRn due to differences in packing.³⁷

Analyses of the pH-dependence of the interactions of the mutated FcRn species indicate that all mutants retain pH-dependence (significantly stronger binding at pH 6.0 than at pH 7.3). This suggests that the interaction of His436 at position 436 of IgG with Glu137 of FcRn does not make a major contribution to the pH-dependence of the interaction. Significantly, interactions of all FcRn species with mouse IgG2b are less pH-dependent than those with other mouse IgGs. This is consistent with earlier analyses of the rat FcRn–mouse IgG2b interaction,⁴⁰ and is most likely due to the presence of tyrosine rather than histidine at IgG position 435. This lower level of pH-dependence might account for the shorter serum persistence of mouse IgG2b relative to mouse IgG1/IgG2a,^{44,45} despite the similar affinities of the interactions of these two IgGs with mouse FcRn at pH 6.0 (Table 3).

In summary, we have shown that it is possible to generate a mutated human FcRn molecule that binds to heterologous IgGs with which the parent, wild-type FcRn does not interact with a measurable affinity. The effects of mutations of other FcRn residues in the vicinity of the putative human FcRn–IgG interaction site have been analyzed, and indicate that the contribution of IgG residue 436–FcRn residue 137 can vary depending on the nature of proximal residues. Finally, our studies have relevance to understanding human FcRn function, which, in turn, relates to the engineering of optimized antibodies for therapy.

Materials and Methods

Generation of plasmids for expression of mutated human FcRn

The plasmid DNA of human FcRn in pEGFP-N1²⁴ was used as a template for splicing by overlap extension⁴⁶ to generate the mutated variants of human FcRn shown in Table 1. Mutated genes were subcloned as BglIII–BamHI (sites that flank the mutated regions in the human FcRn gene¹⁸) fragments into pAcUW51 vector derivatives containing either the murine β 2m gene⁴⁷ or human β 2m gene²⁴ to generate the following mutants: L137E, D132E/L137E, L137E/loop79–89, L137E/loop121–132 and loop79–89 (Table 1). Clones harboring plasmid constructs with the desired orientation of the gene fragments were sequenced using an ABI PRISM model 3100.

Expression and purification of recombinant FcRn

Recombinant wild-type and mutated FcRn (human) or wild-type mouse FcRn were expressed in insect cells (High-5; Invitrogen) infected with recombinant baculoviruses as described.^{22,47} Recombinant viral stocks were produced by co-transfection of 2×10^6 Sf9 cells with 0.15 μ g of Baculogold DNA (Pharminogen) and 10 μ g of

plasmid DNA in Grace's medium with Cellfectin (Gibco). Third passage virus stocks were used to infect High-5 cells grown in Excell-405 (JRH Biosciences) or Express Five SFM (Invitrogen) to a density of 1×10^6 /ml in suspension at 27 °C. Following infection, High-5 cells were grown at 23–24 °C and supernatant was harvested 72 hours later. Recombinant protein was purified from the supernatant using Ni²⁺-NTA-agarose resin (Qiagen) as described.⁴⁷ Aggregates were removed by subsequent purification using high-performance liquid chromatography and a HiLoad 26/60 Superdex™ 200 prep grade (Pharmacia) column.

Antibodies

HuLys10⁴⁸ and RFB4 [anti-CD22⁴⁹] were used as a source of human and mouse IgG1 (both κ), respectively. HuLys10 is a humanized antibody that recognizes hen egg-white lysozyme (HEL) and was purified from cell-culture supernatants using HEL-Sepharose.⁴⁸ The cell line was a generous gift of Dr Jeff Foote (Fred Hutchinson Cancer Center, Seattle). Mouse IgG2a and IgG2b were purchased from Zymed and eBioscience, respectively.

Binding studies using surface plasmon resonance

SPR experiments were carried out using a BIAcore 2000. Flow-cells of CM5 chips were coupled with human IgG1 (HuLys10), mouse IgG1 (RFB4), mouse IgG2a and mouse IgG2b using amine coupling chemistry. Reference flow-cells were coupled with buffer only during the coupling cycle. For the interactions analyzed in this study, several experiments were run with different chips, different batches of FcRn, different analyte concentration ranges etc. and the coupling densities for the data shown are indicated in the Figure legends. Wild-type or mutated FcRn were injected over the flow-cells at a flow-rate of 10 μ l/minute at 25 °C. For interactions with equilibrium dissociation constants (K_D) in the range of 2 μ M or less, two or three blocks of injections were carried out for each FcRn species using an analogous approach described previously to minimize artifacts due to loss of ligand activity during the course of the experiment.³⁹ For these experiments, FcRn was injected at concentrations ranging from 0.05 μ M to 4 μ M. However, for dissociation constants that ranged from ~ 5 μ M to 30 μ M, the high concentrations of analyte needed (~ 1 –30 μ M) to obtain reliable constants precluded the implementation of the method utilizing multiple blocks of injections. For these interactions, duplicate injections at different times were carried out to assess loss of ligand activity during the course of the experiment. Data analyses for these lower-affinity interactions indicated that the loss of ligand activity was minimal compared with the effect of changes in analyte concentration on equilibrium binding signals. For all experiments, phosphate buffered saline (PBS) at pH 6.0 or pH 7.3 with 0.01% (v/v) Tween 20 and 0.02% (w/v) NaN₃ was used as running buffer. For analyte injections carried out at pH 6.0, the same buffer at pH 7.2 was used to "strip" the flow-cells at the end of each dissociation phase. Data were zero adjusted and reference cell subtracted and analyzed using an approach developed by Ober & Ward,³⁹ or Scatchard analyses with custom-written software. In cases where the affinities at pH 6.0 were clearly very low from the equilibrium

binding levels, the equation:

$$R_D = [\text{analyte}_x](R_{\max} - R_{\text{eqx}})/R_{\text{eqx}}$$

was used to verify that they were greater than 50 μM (R_{\max} is the signal level when all ligand-binding sites are occupied; R_{eqx} is the signal level at equilibrium for a known concentration of analyte, x). Similar analyses could not be carried out for binding data obtained at pH 7.3, as R_{\max} could not be determined at this pH (due to poor binding of all FcRn species at this pH).

Acknowledgements

We are indebted to Jing Tan for expert technical assistance. This work was supported, in part, by funds from the National Institutes of Health (RO1 AI39167 and RO1 GM58538).

References

- Rodewald, R. (1980). Distribution of immunoglobulin G receptors in the small intestine of the young rat. *J. Cell Biol.* **85**, 18–32.
- Rodewald, R. & Abrahamson, D. R. (1982). Receptor-mediated transport of IgG across the intestinal epithelium of the neonatal rat. *Ciba. Found. Symp.*, 209–232.
- Ghetie, V., Hubbard, J. G., Kim, J. K., Tsen, M. F., Lee, Y. & Ward, E. S. (1996). Abnormally short serum half-lives of IgG in beta 2-microglobulin-deficient mice. *Eur. J. Immunol.* **26**, 690–696.
- Junghans, R. P. & Anderson, C. L. (1996). The protection receptor for IgG catabolism is the beta2 microglobulin-containing neonatal intestinal transport receptor. *Proc. Natl Acad. Sci. USA*, **93**, 5512–5516.
- Israel, E. J., Wilsker, D. F., Hayes, K. C., Schoenfeld, D. & Simister, N. E. (1996). Increased clearance of IgG in mice that lack beta 2-microglobulin: possible protective role of FcRn. *Immunology*, **89**, 573–578.
- Ghetie, V. & Ward, E. S. (1997). FcRn: the MHC class I-related receptor that is more than an IgG transporter. *Immunol. Today*, **18**, 592–598.
- Ward, E. S., Zhou, J., Ghetie, V. & Ober, R. J. (2003). Evidence to support the cellular mechanism involved in serum IgG homeostasis in humans. *Int. Immunol.* **15**, 1–9.
- Ellinger, I., Schwab, M., Stefanescu, A., Hunziker, W. & Fuchs, R. (1999). IgG transport across trophoblast-derived BeWo cells: a model system to study IgG transport in the placenta. *Eur. J. Immunol.* **29**, 733–744.
- McCarthy, K. M., Yoong, Y. & Simister, N. E. (2000). Bidirectional transcytosis of IgG by the rat neonatal Fc receptor expressed in a rat kidney cell line: a system to study protein transport across epithelia. *J. Cell Sci.* **113**, 1277–1285.
- Praetor, A., Ellinger, I. & Hunziker, W. (1999). Intracellular traffic of the MHC class I-like IgG Fc receptor, FcRn, expressed in epithelial MDCK cells. *J. Cell Sci.* **112**, 2291–2299.
- Antohe, F., Radulescu, L., Gafencu, A., Ghetie, V. & Simionescu, M. (2001). Expression of functionally active FcRn and the differentiated bidirectional transport of IgG in human placental endothelial cells. *Hum. Immunol.* **62**, 93–105.
- Dickinson, B. L., Badizadegan, K., Wu, Z., Ahouse, J. C., Zhu, X., Simister, N. E. *et al.* (1999). Bidirectional FcRn-dependent IgG transport in a polarized human intestinal epithelial cell line. *J. Clin. Invest.* **104**, 903–911.
- Kobayashi, N., Suzuki, Y., Tsuge, T., Okumura, K., Ra, C. & Tomino, Y. (2002). FcRn-mediated transcytosis of immunoglobulin G in human renal proximal tubular epithelial cells. *Am. J. Physiol. Renal Physiol.* **282**, F358–F365.
- Spiekermann, G. M., Finn, P. W., Ward, E. S., Dumont, J., Dickinson, B. L., Blumberg, R. S. & Lencer, W. I. (2002). Receptor-mediated immunoglobulin G transport across mucosal barriers in adult life: functional expression of FcRn in the mammalian lung. *J. Exptl Med.* **196**, 303–310.
- Cianga, P., Medesan, C., Richardson, J. A., Ghetie, V. & Ward, E. S. (1999). Identification and function of neonatal Fc receptor in mammary gland of lactating mice. *Eur. J. Immunol.* **29**, 2515–2523.
- Borvak, J., Richardson, J., Medesan, C., Antohe, F., Radu, C., Simionescu, M. *et al.* (1998). Functional expression of the MHC class I-related receptor, FcRn, in endothelial cells of mice. *Int. Immunol.* **10**, 1289–1298.
- Ghetie, V. & Ward, E. S. (2000). Multiple roles for the major histocompatibility complex class I-related receptor FcRn. *Annu. Rev. Immunol.* **18**, 739–766.
- Story, C. M., Mikulska, J. E. & Simister, N. E. (1994). A major histocompatibility complex class I-like Fc receptor cloned from human placenta: possible role in transfer of immunoglobulin G from mother to fetus. *J. Exptl Med.* **180**, 2377–2381.
- Simister, N. E., Story, C. M., Chen, H. L. & Hunt, J. S. (1996). An IgG-transporting Fc receptor expressed in the syncytiotrophoblast of human placenta. *Eur. J. Immunol.* **26**, 1527–1531.
- Kristoffersen, E. K. & Matre, R. (1996). Co-localization of the neonatal Fc gamma receptor and IgG in human placental term syncytiotrophoblasts. *Eur. J. Immunol.* **26**, 1668–1671.
- Leach, J. L., Sedmak, D. D., Osborne, J. M., Rahill, B., Lairmore, M. D. & Anderson, C. L. (1996). Isolation from human placenta of the IgG transporter, FcRn, and localization to the syncytiotrophoblast: implications for maternal-fetal antibody transport. *J. Immunol.* **157**, 3317–3322.
- Firan, M., Bawdon, R., Radu, C., Ober, R. J., Eaken, D., Antohe, F. *et al.* (2001). The MHC class I related receptor, FcRn, plays an essential role in the maternofetal transfer of gammaglobulin in humans. *Int. Immunol.* **13**, 993–1002.
- Claypool, S. M., Dickinson, B. L., Yoshida, M., Lencer, W. I. & Blumberg, R. S. (2002). Functional reconstitution of human FcRn in Madin-Darby canine kidney cells requires co-expressed human beta 2-microglobulin. *J. Biol. Chem.* **277**, 28038–28050.
- Ober, R. J., Radu, C. G., Ghetie, V. & Ward, E. S. (2001). Differences in promiscuity for antibody-FcRn interactions across species: implications for therapeutic antibodies. *Int. Immunol.* **13**, 1551–1559.
- Kim, J. K., Tsen, M. F., Ghetie, V. & Ward, E. S. (1994). Localization of the site of the murine IgG1 molecule that is involved in binding to the murine intestinal Fc receptor. *Eur. J. Immunol.* **24**, 2429–2434.
- Burmeister, W. P., Huber, A. H. & Bjorkman, P. J.

- (1994). Crystal structure of the complex of rat neonatal Fc receptor with Fc. *Nature*, **372**, 379–383.
27. Medesan, C., Matesoi, D., Radu, C., Ghetie, V. & Ward, E. S. (1997). Delineation of the amino acid residues involved in transcytosis and catabolism of mouse IgG1. *J. Immunol.* **158**, 2211–2217.
 28. Kim, J. K., Firan, M., Radu, C. G., Kim, C. H., Ghetie, V. & Ward, E. S. (1999). Mapping the site on human IgG for binding of the MHC class I-related receptor, FcRn. *Eur. J. Immunol.* **29**, 2819–2825.
 29. Martin, W. L., West, A. P. J., Gan, L. & Bjorkman, P. J. (2001). Crystal structure at 2.8 Å of an FcRn/heterodimeric Fc complex: mechanism of pH dependent binding. *Mol. Cell*, **7**, 867–877.
 30. Dall'Acqua, W., Woods, R. M., Ward, E. S., Palaszynski, S. R., Patel, N. K., Brewah, Y. A. *et al.* (2002). Increasing the affinity of a human IgG1 to the neonatal Fc receptor: biological consequences. *J. Immunol.* **169**, 5171–5180.
 31. Frodin, J. E., Lefvert, A. K. & Mellstedt, H. (1990). Pharmacokinetics of the mouse monoclonal antibody 17-1A in cancer patients receiving various treatment schedules. *Cancer Res.* **50**, 4866–4871.
 32. Saleh, M. N., Khazaeli, M. B., Wheeler, R. H., Dropcho, E., Liu, T., Urist, M. *et al.* (1992). Phase I trial of the murine monoclonal anti-GD2 antibody 14G2a in metastatic melanoma. *Cancer Res.* **52**, 4342–4347.
 33. Ahouse, J. J., Hagerman, C. L., Mittal, P., Gilbert, D. J., Copeland, N. G., Jenkins, N. A. & Simister, N. E. (1993). Mouse MHC class I-like Fc receptor encoded outside the MHC. *J. Immunol.* **151**, 6076–6088.
 34. Simister, N. E. & Mostov, K. E. (1989). An Fc receptor structurally related to MHC class I antigens. *Nature*, **337**, 184–187.
 35. Kabat, E. A., Wu, T. T., Perry, H. M., Gottesman, K. S. & Foeller, C. (1991). *Sequences of Proteins of Immunological Interest*, Department of Health and Human Services, Bethesda, MD.
 36. Sanchez, L. M., Penny, D. M. & Bjorkman, P. J. (1999). Stoichiometry of the interaction between the major histocompatibility complex-related Fc receptor and its Fc ligand. *Biochemistry*, **38**, 9471–9476.
 37. West, A. P. J. & Bjorkman, P. J. (2000). Crystal structure and immunoglobulin G binding properties of the human major histocompatibility complex-related Fc receptor. *Biochemistry*, **39**, 9698–9708.
 38. Schuck, P., Radu, C. G. & Ward, E. S. (1999). Sedimentation equilibrium analysis of recombinant mouse FcRn with murine IgG1. *Mol. Immunol.* **36**, 1117–1125.
 39. Ober, R. J. & Ward, E. S. (2002). Compensation for loss of ligand activity in surface plasmon resonance experiments. *Anal. Biochem.* **306**, 228–236.
 40. Raghavan, M., Bonagura, V. R., Morrison, S. L. & Bjorkman, P. J. (1995). Analysis of the pH dependence of the neonatal Fc receptor/immunoglobulin G interaction using antibody and receptor variants. *Biochemistry*, **34**, 14649–14657.
 41. Vaughn, D. E., Milburn, C. M., Penny, D. M., Martin, W. L., Johnson, J. L. & Bjorkman, P. J. (1997). Identification of critical IgG binding epitopes on the neonatal Fc receptor. *J. Mol. Biol.* **274**, 597–607.
 42. Shields, R. L., Namenuk, A. K., Hong, K., Meng, Y. G., Rae, J., Briggs, J. *et al.* (2001). High resolution mapping of the binding site on human IgG1 for Fc gamma RI, Fc gamma RII, Fc gamma RIII, and FcRn and design of IgG1 variants with improved binding to the Fc gamma R. *J. Biol. Chem.* **276**, 6591–6604.
 43. Jarvis, D. L. & Finn, E. E. (1995). Biochemical analysis of the N-glycosylation pathway in baculovirus-infected Lepidopteran insect cells. *Virology*, **212**, 500–511.
 44. Pollock, R. R., French, D. L., Metlay, J. P., Birshtein, B. K. & Scharff, M. D. (1990). Intravascular metabolism of normal and mutant mouse immunoglobulin molecules. *Eur. J. Immunol.* **20**, 2021–2027.
 45. Vieira, P. & Rajewsky, K. (1988). The half-lives of serum immunoglobulins in adult mice. *Eur. J. Immunol.* **18**, 313–316.
 46. Horton, R. M., Hunt, H. D., Ho, S. N., Pullen, J. K. & Pease, L. R. (1989). Engineering hybrid genes without the use of restriction enzymes: gene splicing by overlap extension. *Gene*, **77**, 61–68.
 47. Popov, S., Hubbard, J. G., Kim, J., Ober, B., Ghetie, V. & Ward, E. S. (1996). The stoichiometry and affinity of the interaction of murine Fc fragments with the MHC class I-related receptor, FcRn. *Mol. Immunol.* **33**, 521–530.
 48. Foote, J. & Winter, G. (1992). Antibody framework residues affecting the conformation of the hypervariable loops. *J. Mol. Biol.* **224**, 487–499.
 49. Campana, D., Janossy, G., Bofill, M., Trejdosiewicz, L. K., Ma, D., Hoffbrand, A. V. *et al.* (1985). Human B cell development. I. Phenotypic differences of B lymphocytes in the bone marrow and peripheral lymphoid tissue. *J. Immunol.* **134**, 1524–1530.

Edited by I. Wilson

(Received 25 April 2003; received in revised form 16 July 2003; accepted 17 July 2003)